Seismic behaviour of wood-concrete frame shear-wall system and comparison with code provisions

Luca Pozza, Roberto Scotta
University of Padova, Italy

Andrea Polastri, Ario Ceccotti
CNR – IVALSA San Michele all'Adige, Italy

Abstract: Constructive systems adopting mixed shear walls made of a wood frame and fibrous or cementitious sheets are largely spread nowadays, particularly for prefabricated buildings. The use of gypsum boards as bracing panels is already widespread, but also fiber cement or reinforced concrete slabs can be used. The choice of such different materials allows to reach excellent thermal and acoustic insulation performance. Perhaps the demonstration of their sound structural behavior, especially towards the earthquake resistance is still to be given, and their ductility and dissipative capacities still need to be fully assessed even if some experimental tests have already been conducted. Moreover these particular constructive systems are yet not accounted in the building codes (Eurocode 5, EN 1995 [1] and Eurocode 8, EN 1998 [2]) and no guidelines are given for their seismic design in order to assure an adequate overstrength of the bracing panels and the adequacy of the fixing system of the panels to the wooden frames.

1 Introduction

The investigated mixed constructive system combines a typical platform frame building system with an thin external reinforced concrete board acting as a diaphragm against the horizontal forces and having also thermal and acoustic functions. A building made by the use of this mixed wood-reinforced concrete walls is a precast modular system where the wall panels are preassembled in the factory; on the construction site the single precast modular panel is then assembled connecting the adjacent panel with screws and to the foundation with mechanical fasteners (nailed holdown and bolts). The structural layout is similar to that of platform framing system. The walls are made of modular panels having a typical aspect ratio of 3:1 (3.24m high and 1.08m long). A scketch of a single panel is presented in Figure 1. The particular arrangement of the OSB panels and concrete slabs provides a continous ventilation cavity from fondation to the roof. The presece of this continous air layer between the two diaphragms guarantees an optimal thermo-hygrometric performance and keeps dry the wood-concrete interface avoiding the deterioration of wood. Two resistant systems with different structural functions can be identified within a modular panel: elements that carry the vertical actions and elements which react to the horizontal actions (wind and earthquake).

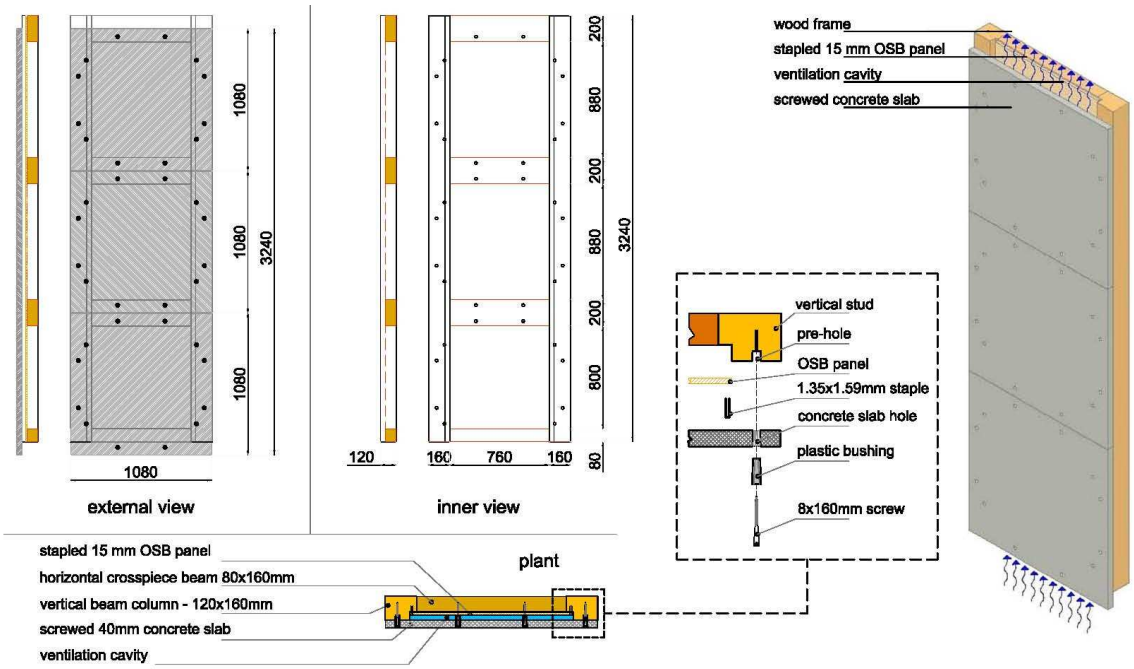

Fig. 1 View of the precast modular panel

The system loaded by the vertical loads is a wood frame structure which transfers to the foundation the vertical load (structural weight). Two adjacent modular wall panels are jointed together by the use of a vertical joint cover screwed to the vertical studs. This joint cover achives the vertical support for the floor and roof beams.

Bracing system reacting to horizontal actions consists of two different diaphragms connected to wood frame. The first is made of three OSB panels (1080 mm x 1080 mm x 15 mm) connected with staples to the wood frame. The second consists of three square reinforced concrete board (1080 mm x 1080 mm x 40 mm). The reinforcement of the slabs is made of wire mesh knitted 60mm x 60 mm. The concrete slab is fixed to the wood frame using 8 mm diameter screws coupled with a plastic bushing. The plastic bushing serves several important functions: reduces the clearance between the concrete slab and the screw without using sealant products; acts as spacer between the horizontal transverse beams of the wood frame and the concrete board ensuring the ventilation cavity; increases bearing resistance of the screws.

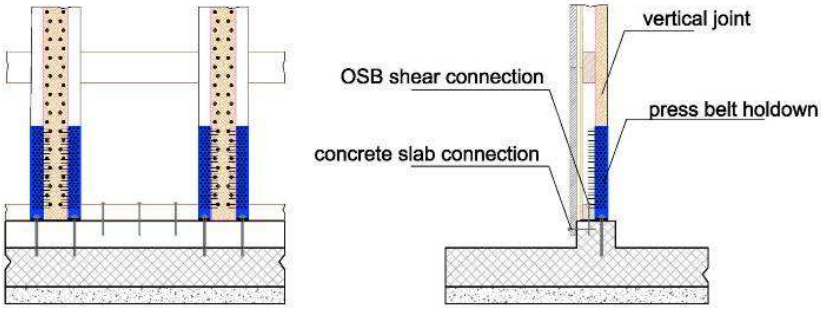

Fig. 2 View of the foundation anchor system

The modular wall panel is anchored to the foundations using special holdowns and bolts in order to avoid the roking and the slip effect respectively. The holdown is made by press bent L-profile 3 mm thick nailed at the corner formed by the vertical columns and the joint cover element. This holdown is connected to the concrete foundation with mechanical or chemical fixings as standard. The wall panel slip is prevented by fixing the bottom plate

and the concrete slab to the foundation by bolts. The shear action of OSB bracing is transferred to the foundation by anchors between the bottom horizontal beam to the concrete slab, Figure 2.

2 Quasi static cyclic and monotonic test

In order to verify the effective resistant characteristics and the hysteretic behaviour of the investigated constructive system a series of experimental tests were performed. This paragraph describes the structural layout and the main characteristics of the tested walls with details about the connectors and bracing system. Test layout, instrumentation, load condition and protocol use during the cyclic test are also given. The outcomes from quasi static reversed cyclic tests are reported. Finally a comparison between this experimental results and the code provisions are given and critically discussed.

2.1 Test wall configuration

Three different configuration of walls were tested: “Wall A” with a ratio of 3:1 (3.24m high and 1.08m long, one modular panel); “Wall B” aspect ratio of 3:2 (3.24m high and 2.16m long made with two adjacent modular panel) and “Wall C”, with a ratio of 1:1 which presents an window opening in the central panel, (3.24m high and 3.24 m long made of three adjacent modular panel). In sake of brevity only the outcomes from the test of "Wall B" and "Wall C" are hereafter given.

2.2 Test setup and instrumentation

“Wall B” and “Wall C” were tested using different setups due to their different geometrical characteristics and load conditions. In order to faithfully reproduce the actual base connection system a base concrete foundation was provided.

The test setup used for “Wall B” is presented in Figure 3. Vertical load equal to 20 kN/m was applied using three hydraulic actuators placed on the vertical wood columns. To allow the wall uplift without variance in the vertical load the hydraulic actuators were placed in series with a spring. The “Wall C” test was carried out loading two walls arranged specular respect to load axis with the aim of balancing the torsional effects and to keep the unidirectional movement of the wall. The setup used for “Wall C” is presented in Figure 3. Lateral guides with rollers in contact to the top horizontal plate were also used to ensure unidirectional movement of the walls. Uniform vertical load equal to 20 kN/m was applied at the top of the wall through actuators and a distribution steel beam. The displacements of the wall panel were measured with transducers placed as shown in Figure 3.

2.3 Test procedure

The cyclic tests were performed according to EN 12512 [3] in displacement control at rate of 0.04 mm/s. The yielding displacement, v_y, was estimated referring to preliminary test made on single modular panel "Wall A". The collapse of the wall has not been reached during the cyclic tests stopped at 80 mm displacement cycles. To verify the actual lateral load capacity and ductility of the investigated constructive system, a ramp monotonic test on the “Wall C” was performed according to EN 26891 [4] in displacement control at a rate of 0.04mm/s.

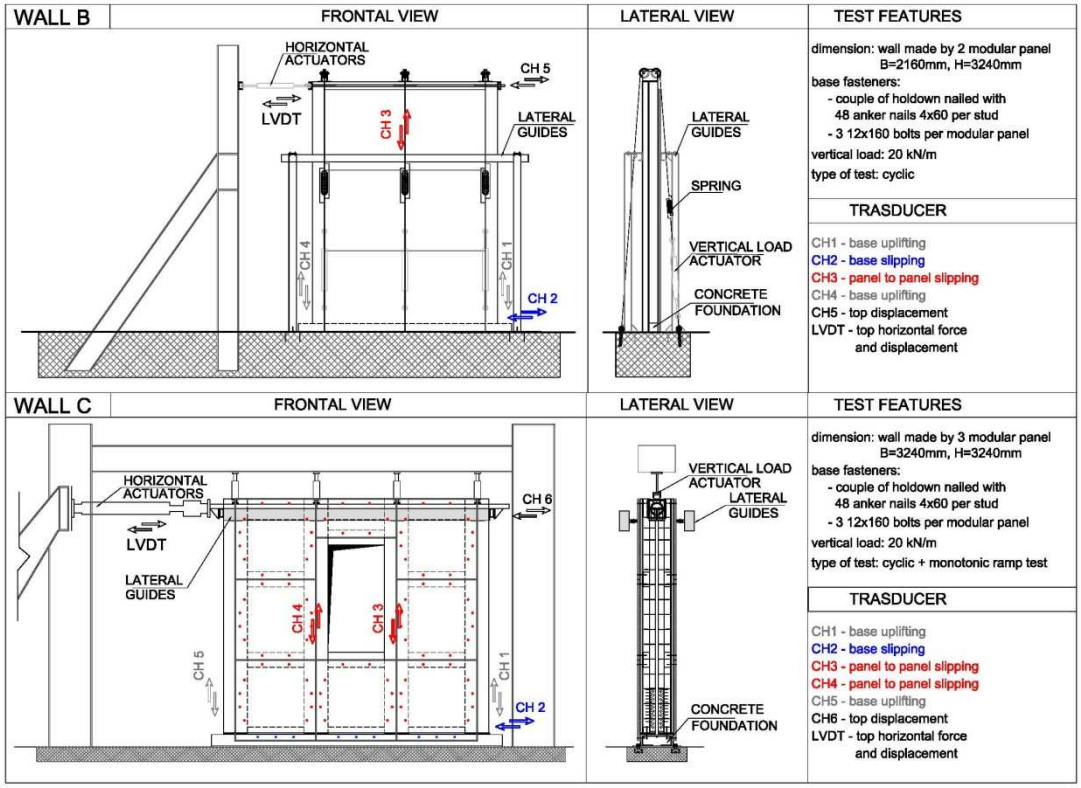

Fig. 3 Sketch of the setup, "Wall B" and "Wall C"

2.4 Test outcomes

The performed cyclic tests allowed to define the hysteretic cycles of the walls obtained plotting the measured top displacement and the force imposed by the actuator, Figure 3. As shown in Figure 4, the load-slip curve related to "Wall B" is asymmetric because during the test the lateral guides have shown problems in the maintenance of the unidirectional movement of the wall. Due to this problem it has not been possible to carry out the last push cycles but only those in pull. At the largest cycle amplitude admitted by the actuator system (100mm) the wall has not jet reached the failure.

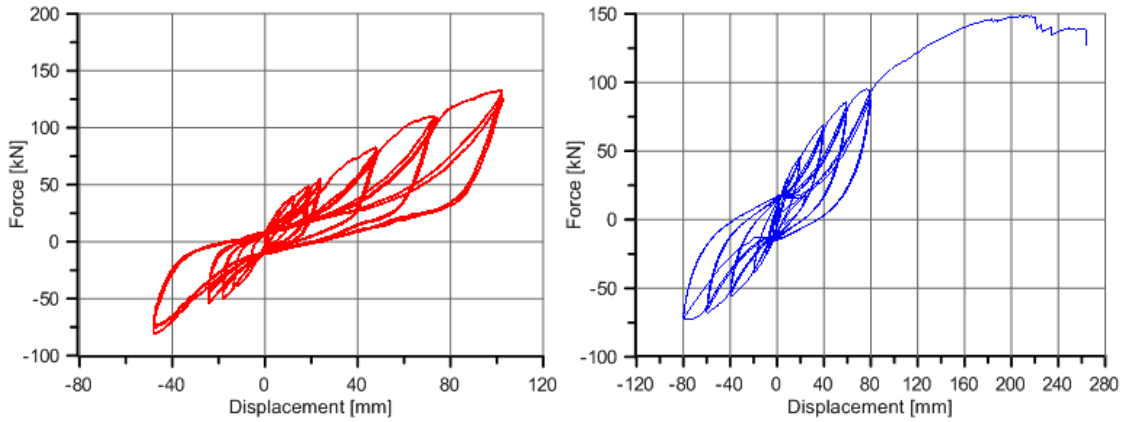

Fig. 4. Load displacement curve, cyclic test for "Wall B" (left) and "Wall C" (right)

During the cyclic test, the "Wall C" has not shown failure or relevant strength degrading phenomena. The collapse condition was achieved only with a monotonic ramp test performed at the end of the cyclic test as shown Figure 4. "Wall B" and "Wall C" present the typical hysteretic behaviour of the steel-wood and wood-wood connections characterized by the pinching phenomenon. Moreover the tested walls show a marked

hardening phase due to the use of large diameter connectors to fix the concrete bracing system to the wood frame.

Fig. 5. Wall configuration at the end of the test

2.4.1 Determination of stiffness, yielding point and ductility

The yielding condition can be define according to EN 12512 [3], but in the studied case, because of the strong hardening behavior of the load-slip curve, this approach is not correct. Consequently, also the calculated ductility values results are unrepresentative of the actual displacement capacity of wall.

In this work, an alternative approach was used in order to obtain a more accurate prediction of yield conditions. The exponential approximation of the monotonic curve proposed monotonic curve proposed by Folz and Filiatrault [5] was used according to (1).

$$F=(r_1 k_0 x+F_0)(1-e^{\frac{-k_0 x}{F_0}}) \quad (1)$$

where:
F = actual value of the force
x = actual value of the displacement
k_0 = elastic stiffness
$r_1 k_0 = \beta$ = hardening stiffness
F_0 = residual force

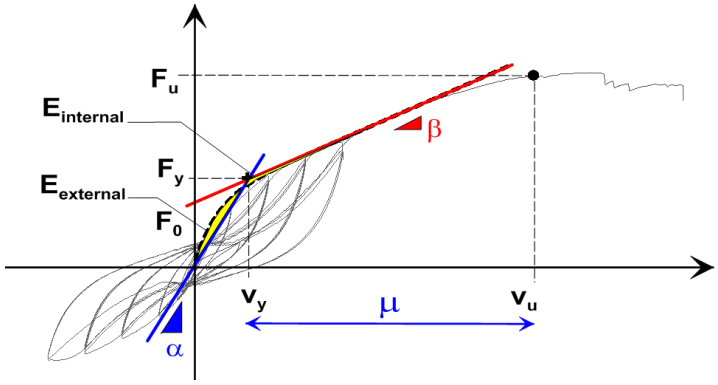

Fig. 6. Identification of yelding point and stiffness on the experimental curve

The stiffness β of the hardening branch and the residual force F_0 are obtained fitting to the experimental curve while the elastic stiffness α is obtained imposing the equality of the strain energy as depicted in Figure 6. Using an analytical expression for the monotonic

load-displacement curve approximation it is possible to evaluate the compensation area, representing the strain energy, through equation (2), (3) and (4).

$$E_{\_internal} = \int_0^{\chi} [(r_1 k_0 x + F_0)(1 - e^{\frac{-k_0 x}{F_0}}) - \alpha x] dx \quad (2)$$

$$E_{\_esxternal} = \int_{\chi}^{\infty} [(r_1 k_0 x + F_0) e^{\frac{-k_0 x}{F_0}}] dx \quad (3)$$

The elastic stiffness α is obtained imposing the equality according to Eq. 4.

$$\alpha = \frac{k_0^{\,2}}{2(k_0 + r_1 k_0)} + r_1 k_0 \quad (4)$$

Once the value of the elastic stiffness α is defined the yielding condition (V_y, F_y) is given by the intersection between the elastic and the hardening slope. According to this approach the main outcomes in terms of strength, stiffness and ductility for the tested walls are summarised in Table 1. A comparison with the value obtained from the EN12512 [3] procedure is also given.

Table 1. Test results and interpretation according to exponential and EN 12512 approach

	WALL B		WALL C	
	Test Results		Test Results	
K_0 [kN/mm]	7.9		8.2	
V_u [mm]	102		180	
F_u [kN]	132		145	
	Exp. Approach	EN 12512	Exp. Approach	EN 12512
α [kN/mm]	3.3	5.5	2.6	4.5
β [kN/mm]	1	1	0.6	0.6
V_y [mm]	15.3	7.8	23.3	11.5
F_y [kN]	50.9	42.8	59.8	51.7
μ	6.7	13.1	7.7	15.7

The results reported in Table 1 confirm that the exponential approach gives reasonable values for the elastic stiffness and of the ductility, as opposed to the ductility values obtained with the UNI 12512 [3] approach, that are too high and inadequate to represent the actual displacement capacity of this building system.

2.4.2 Wall equivalent viscous damping and empairment strength

The equivalent viscous damping, ν_{eq}, is an adimensional parameter useful to summarize the hysteretic properties of a structural element. It is define according to EN 12512 [3], referring to the 3rd cicle of each ductility level, as reported in the following Table 2.

The equivalent viscous damping values decrease with the increasing of cycle amplitude. This aspect means a reduction in the dissipative capability with the increasing of the displacement due to the pinching phenomenon. However, it should be stressed that the equivalent viscous damping is always greater than 7%, confirming the good dissipative capability of this building system.

The strength degrading is a relevant parameter to identify the seismic behaviour of a building system. EC8 [2] uses this parameter to classify the dissipative capability of timber structures and imposes an impairment strength lower than 20% in order to consider a structure as ductile.

Table 2. Equivalent viscous damping values obtained from the cyclic test

Wall B				Wall C			
Cycle amplitude	Ep [kJ]	Ed [kJ]	ν_{eq}	Cycle amplitude	Ep [kJ]	Ed [kJ]	ν_{eq}
18mm	436.5	387	14.12%	10mm	304.6	282	14.74%
24mm	657.48	574	13.90%	20mm	911	721	12.60%
48mm	1971.6	1561	12.61%	40mm	2725.2	1928	11.27%
72mm	3965.4	2250	9.04%	60mm	5128.8	2695	8.37%
102mm	6763.62	3263	7.68%	80mm	7569.6	4030	8.48%

Table 3. Empairment strength at each cycle amplitude

Wall B		Wall C	
Cycle amplitude	Empairment strength	Cycle amplitude	Empairment strength
18mm	0.041	10mm	0.025
24mm	0.047	20mm	0.059
48mm	0.067	40mm	0.078
72mm	0.069	60mm	0.085
102mm	7.10%	80mm	9.50%

As show in Table 3 the empairment strength values are always lower than 10% confirming the good behavior of this construction system under cyclic actions and, therefore, its adequacy for use in seismic zones.

2.5 Comparison with design provisions according to EC5 [1]

In this section a comparison between the outcome of the experimental tests and the design provisions is given with regard to the strength and stiffness value.

The analytical lateral resistance and stiffness of each tested walls are obtained by adding the strength and stiffness values related to the single modular wall panel. The following Figure 7 reports in detail the analytical stiffness and strength of each wall. The modular panel with a window, used in the Wall C, was considered with reduced mechanical characteristics because it had only one entire square panel. Figure 7 reports the experimental load displacement curve, the exponential approximation and the proposed bi-linearization for each tested wall. The analytical estimation of the initial stiffness and of the maximum strength are also reported.

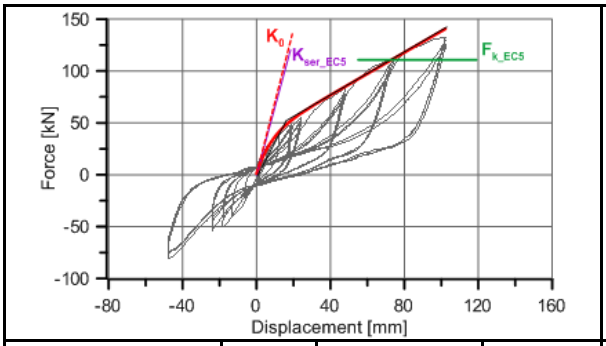

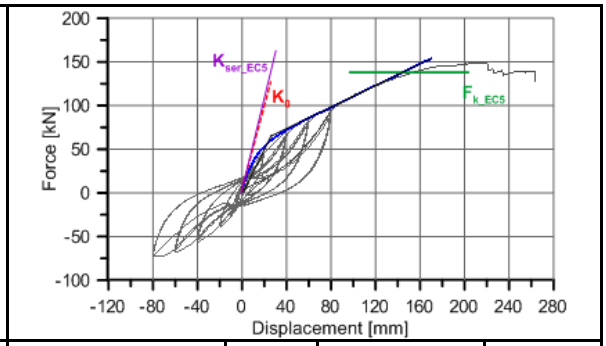

K_0 [kN/mm]	7.92	F_u [kN]	132.03	K_0 [kN/mm]	8.21	F_u [kN]	145.01
K_{ser_EC5} [kN/mm]	7.78	F_{max_EC5} [kN]	113.96	K_{ser_EC5} [kN/mm]	8.94	F_{max_EC5} [kN]	131.05
Δk [%]	1.52%	ΔF [%]	13.67%	Δk [%]	9.02%	ΔF [%]	9.62%

Fig. 7. Comparison between the experimental results and the code provisions

As depicted in Figure 7 the actual value of the lateral resistance is always greater than that obtained with the code provision. The difference is never greater than 15% and it is in line with the ratio between the 5% percentile and the avarege value of a typical normal probabilistich distribution for a wood structure. Regarding to the initial stiffness the analytical values fit very well with the experimental ones: the differences are always lower than 10%.

3 Numerical model of the tested modular panel

The hybrid wood-concrete buildings is characterized by four different bearing systems: bracing systems, hold-downs, base bolts and in plane vertical joints between adjacent precast modules. Regarding to hysteretic behavior, the fasteners used in this building system show a pinched load displacement response and exhibits degradation under cyclic loading. In this work the research-oriented numerical code "Open System for Earthquake Engineering Simulation" was used in order to faithfully reproduce the actual hysteretic behavior of the connectors. The nonlinear element "Pinching4" was used to reproduce the 'pinched' load-deformation response and degradation under cyclic loading. The analytical formulations and the damage models of this nonlinear element are described in [6].

3.1 Modeling of the single connection element

The calibration of the nonlinear element able to reproduce the fasteners behaviour has been made with reference to the load-displacement curves of single connectors obtained from the experimental tests. Figure 8 shows as example the comparison between the experimental cyclic tests on base bolts, hold-down, bracing system and vertical panel to panel connection elements related to "Wall B" and the respective numerical simulations.

The proposed nonlinear numerical model shows the typical pinched behavior in the load-displacement curves, the reduction in stiffness for the reloading cycles and the strength reduction as stated in the initial hypotheses. The numerical results fit well the experimental ones also in terms of energy dissipation, with maximum differences of 12% for the hold down, 8% for the base bolt, 7% for the bracing system and 6% for the panel to panel joint.

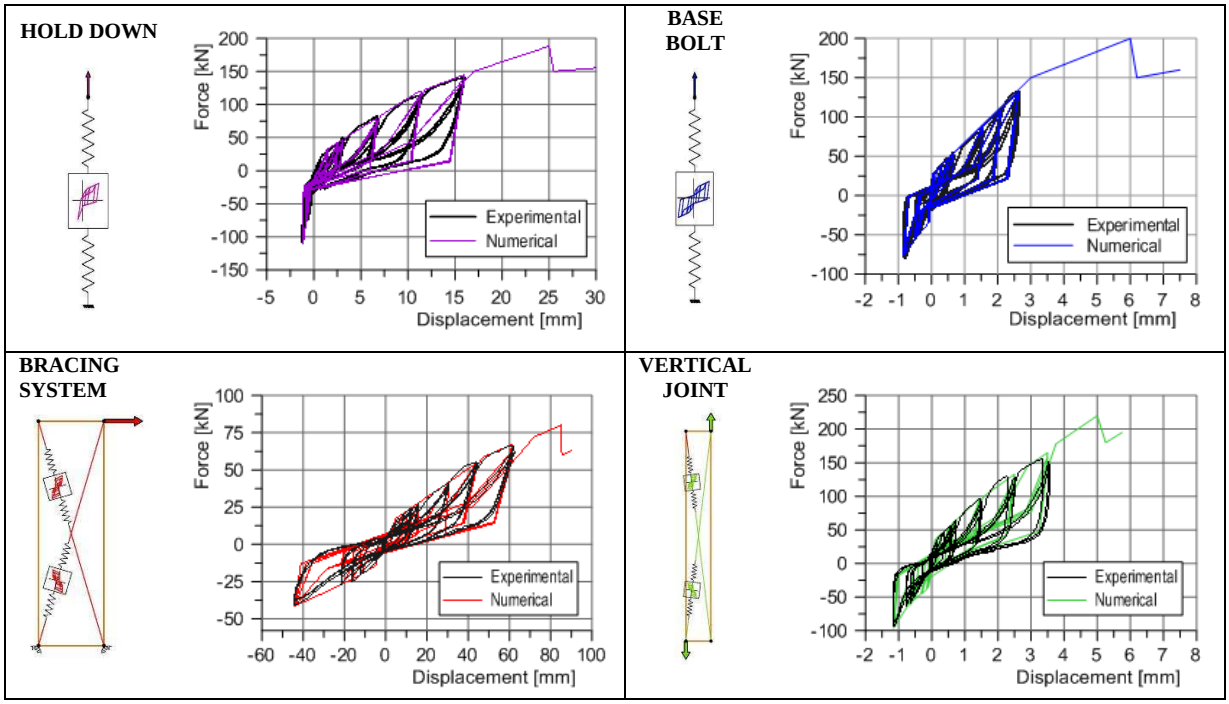

Fig. 8. Comparison between experimental results and numerical load-displacement curve

3.2 Numerical model of the wall,

In order to assess the wall panel-basic joints interaction and the effect of the vertical load, the complete cyclic test on “Wall B” and “Wall C” has been simulated. The numerical model is based on the hypothesis that the nonlinear behavior of the wall is concentrated in the connectors, whereas the wood frame remains in its elastic field. Therefore Finite Element Models consist of a perimeter frame made by stiff elastic truss element braced and connected to the base by the nonlinear spring defined above. The cyclic test has been simulated by imposing a horizontal displacement to the node located on the upper part of the wall. The vertical load was reproduced applying a nodal force on the top of the wall. A sketch of the numerical model used in the analysis is presented in Figure 9.

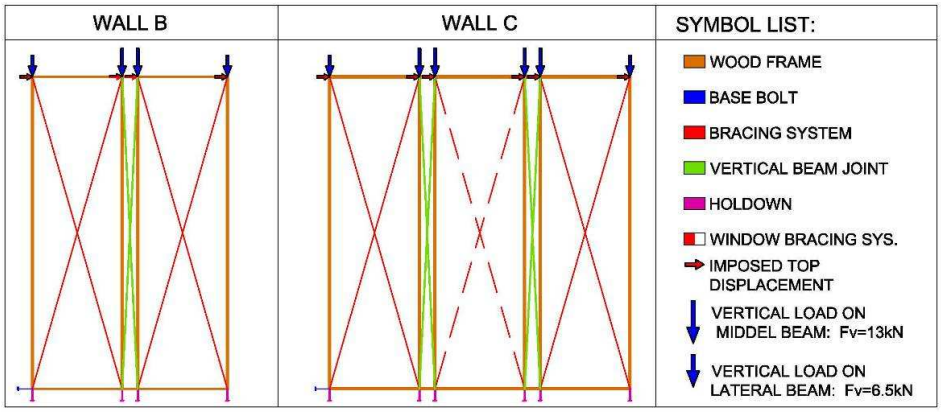

Fig. 9 FEM model “Wall B” (left) and “Wall C” (right)

The load-displacement curve, reported in Figure 10 shows the good correspondence between the results of the experimental test and the numerical simulation at each cycle.

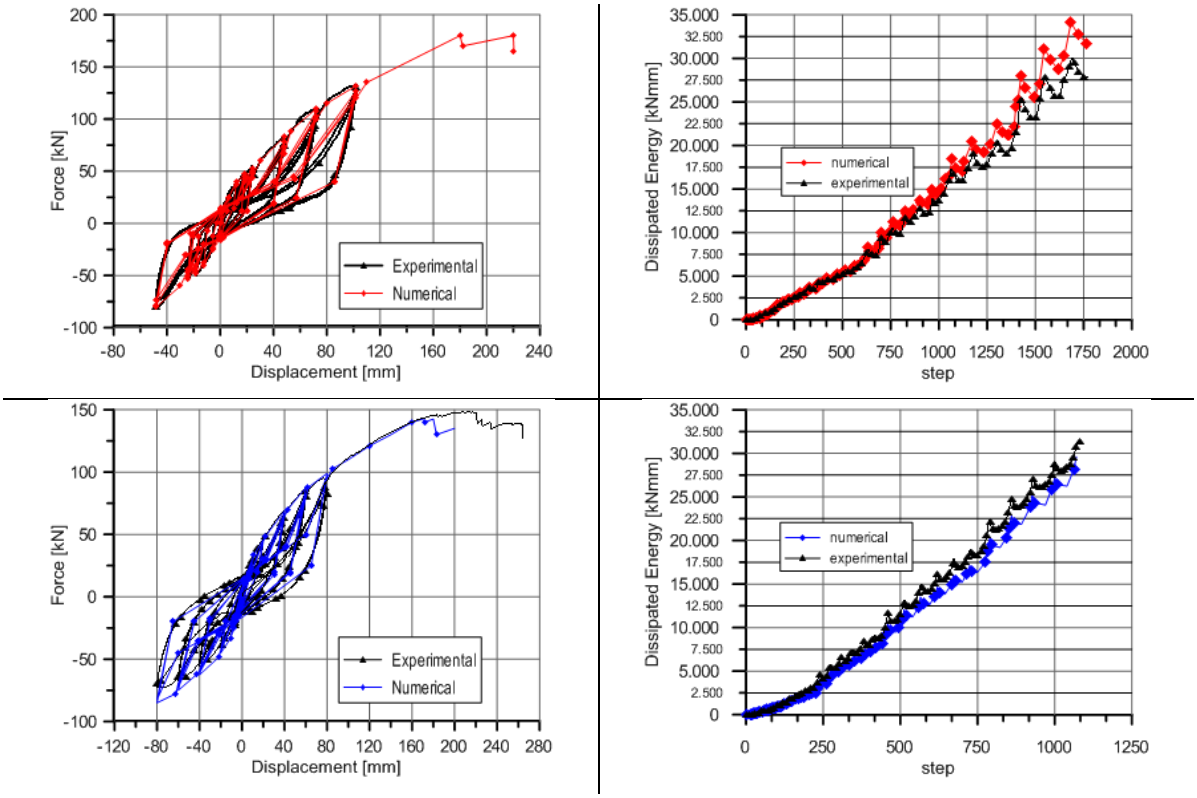

Fig. 10. Comparison between the experimental results and the FEM simulation in terms of load slip curve and dissipated energy “Wall B” (top) and “Wall C” (bottom)

The good quality of the model is further confirmed by the assessment of the dissipated energy: Figure 10 shows the difference in terms of dissipated energy per cycle between the experimental test and the numerical simulation. The correspondence is very good for each cycle amplitude, the maximum difference is 11.5% for “Wall B” and 8.5% for “Wall C”.

4 Assessment of the q-ductility factor

The seismic design of building using FMD method [7] requires the evaluation of the reduction factor q that resumes the post-elastic behavior and the ductility of the building. It should be noted that the definition of the q-factor is not unique since it depends on the criteria used to identify the yielding condition. This condition gives the inelastic seismic design load and, according to the code provisions, EC8 [2], it can be obtained with a properly linearization of the building response, represented through its pushover curve.

4.1 Case study building

In order to define the actual seismic performance of the hybrid constructive system and to make a direct comparison with crosslam one, the same three storey building tested on shaking table during SOFIE project was considered [8]. The B configuration with symmetric opening at the ground floor was investigated. The geometrical layout of this three storey building was compatible with the precast modular wood concrete panel dimension as depicted in Figure 11.

Fig. 11 Case study: modular wall panel arrangement

In this work the analyses focused on the walls placed along the X direction, which present two metre wide opening at the ground floor. Figure 11 reports the studied walls geometry, the fasteners and bracing system arrangement. Two different mass configurations were investigated in order to verify the influence of the main period of vibration on the seismic response of the building. The difference between the two case study in terms of total mass is about 25%. Table 4 reports the storey mass distribution and the eigenfrequency T_1 of each studied building.

Table. 4. Different mass distribution considered

Building	1st storey	2nd storey	3rd storey	Total	T_1
N.1	16.5t	16.5t	12.7t	45.7t	0.48 sec
N.2	10.7t	10.7t	8.4t	29.8t	0.32 sec

4.2 Procedure for q-factor evaluation

The procedure adopted in this work for the q-factor estimation is according to Ceccotti [8] and Pozza et a. [9].

$$q = PGA_{u\_eff.} / PGA_{design} = PGA_{u\_eff.} / PGA_{yielding} \quad (5)$$

4.3 Seismic design of the case study building

In this work it was assumed that the case study building was made by assembling the same modular wall panels subjected to the cyclic tests described in the previous section. The seismic design of the case studied building is based on the lateral shear resistance of the single precast modular panel and consists of the following two steps: evaluation of the base shear resistance F_h according to the outcome of the experimental test and evaluation of the maximum $PGA_{\_design}$ compatible with the base shear resistance adopting a Linear Static Analysis performed considering the following common data according to Eurocode 8 [2] type 1 elastic response spectra and rock foundation (type A soil according to EN 1998-1, corresponding to S=1.0, T_B=0.15sec, T_C=0.4sec, T_D=2.0sec), behavior factor q=1, lowest bound factor for the design spectrum β=0.20 and building importance factor γ_I=1.

Table 5 summarizes the outcomes of the seismic design in terms of maximum $PGA_{\_design}$ values compatible with the base shear resistance of the modular precast panel.

Table 5. Seismic design parameters

Bulding test	Total mass	Fh max	Sd(T1)	$PGA_{\_yielding}$
N.1	45.7t	51.8x4x1.1/1.30=175.3kN	0.39g	0.18g
N.2	29.81	51.8x4x1.1/1.30=175.3kN	0.60g	0.24g

4.4 Seismic design of the case study building

The walls placed along the X direction with two metre wide opening at the ground floor was modelled based on the assumption that the nonlinear behavior of the wall is concentrated in the connectors whereas the wood frame remains in its elastic field. Figure 12 reports a sketch of the numerical model used for the analysis with the indication of the type and position of nonlinear springs and of the storey masses.

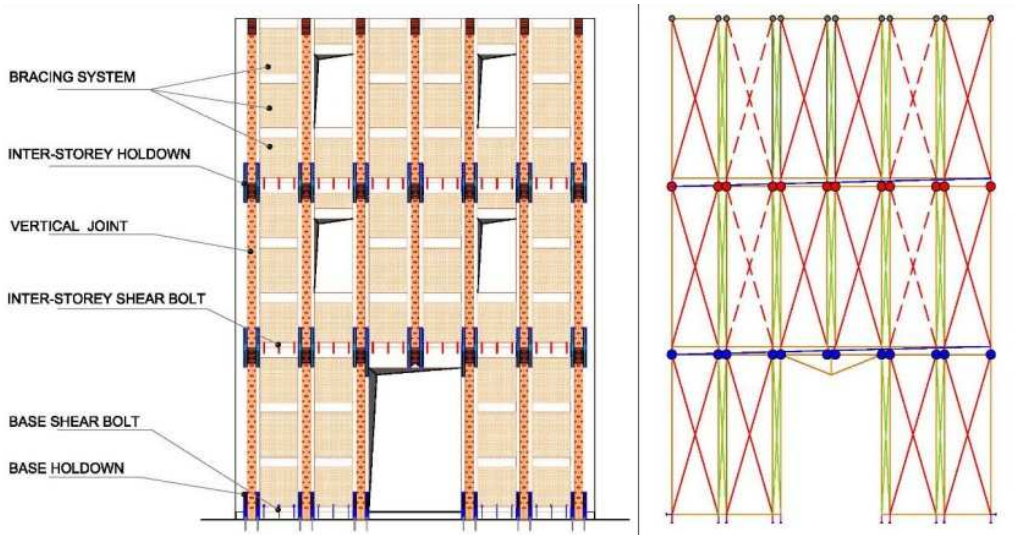

Fig. 12 Investigated wall panels: fasteners and bracing system arrangement (left) and FEM model, type and position of the nonlinear elements (right)

4.5 Evaluation of the q-factor

Using the numerical model above defined, several nonlinear dynamic analysis were performed to evaluate the most suitable q-ductility factor for this wood-concrete system. In order to define the influence of the frequency content of the earthquakes on the building response, a nonlinear dynamic analysis was performed considering 7 different artificially generated seismic shake, so as to meet the spectrum compatibility requirement. The dynamic equilibrium equations have been integrated with a time step of 0.001 second, by adopting an equivalent viscous damping of 2%, according to the Rayleigh model.

Both buildings that were tested have been subjected to a growing level of seismic intensity, from the peak acceleration value equal to PGA_{design} (i.e. $PGA_{yielding}$) to the collapse condition (PGA_{u_eff}) stated as the first achievement of the ultimate displacement of the bracing system or of a base connectors. The near collapse condition was defined with the same criteria reported in [9], e.g. was assumed as an uplift of 25mm for the holdown connections and a shear displacement of the bracing system that leads to a inter storey drift equal to 100mm. Figure 13 reports the PGA_{u_eff} that leads the building to the near collapse condition and the related q factor values for each earthquake considered and for both the case studies respectively.

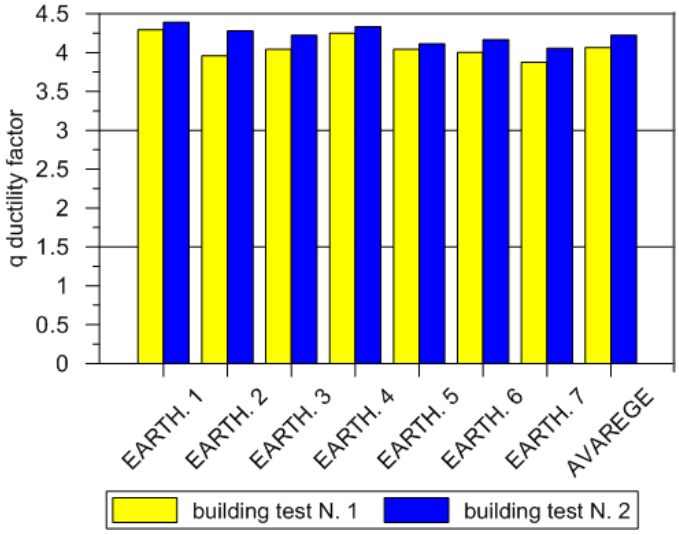

Figure 13. Values of the q-factor for the considered earthquackes

Independently from the approach used the q-ductility factors settle on a value equal to 4 confirming the good dissipative capability of this construction system.

5 Conclusions

In wall structures studied the ductility values are greater than 6, therefore, based on the EC8 [2] provisions this constructive system can be considered as a structure with a high level of ductility. However the design values obtained referring to the code provisions are in concordance with the outcomes form the experimental test. This confirms the adequacy of the code provisions to define the strength and stiffness of the mechanical fasteners used in this mixed wood-concrete constructive system. This constructive system doesn't belong to the standard building typologies reported on table 8.1 of EC8 [2] although it is similar to the Platform Framing technique. However the obtained q-factor value is in line with the code provision that affirm that this constructive system can be classified as high dissipative capability structure.

6 Acnowledgements

The research has been supported by the Polifar s.r.l. Company; the autors would like to thank the tecnical staff of CNR – IVALSA, San Michele all'Adige.

7 References

[1] European Committee for Standardization (CEN). 2004. “Design of timber structures - Part 1-1 General: Common rules for buildings”, Eurocode 5, Standard EN 1995-1-1, Brussels, Belgium.

[2] European Committee for Standardization (CEN), 2004. “Design of structures for earthquake resistance - Part 1 General rules seismic actions and rules for buildings”, Eurocode 8, Standard EN 1998-1, Brussels, Belgium.

[3] European Committee for Standardization (CEN). EN 12512 – Timber structures – Test methods – Cyclic testing of joints made with mechanical fasteners. Brussels, Belgium, 2001.

[4] European Committee for Standardization (CEN). EN 26891, Timber structures – Joints made with mechanical fasteners – General principles for the determination for strength and deformation characteristics. Brussels, Belgium, 1991

[5] Folz, B.,Filiatrault, A. 2004. Seismic analysis of woodframe structures. I: model formulation. Journal of Structural engineering, Vol 130 pp 1353-1360

[6] Fenves G.L., 2005, Annual Workshop on Open System for Earthquake Engineering Simulation, Pacific Earthquake Engineering Research Center, UC Berkeley, http://opensees.berkeley.edu/.

[7] Chopra, AK. Dynamics of structures—theory and applications to earthquake engineering. Upper Saddle River: NJ: Prentice Hall; 1995.

[8] Ceccotti, A. New technologies for construction of medium-rise buildings in seismic regions: the XLAM case. IABSE Struct Eng Internat 2008;18:156–65. Tall Timber Buildings (special ed.).

[9] Pozza, L., Scotta, R., Vitaliani, R. 2009. A non linear numerical model for the assessment of the seismic behaviour and ductility factor of X-lam timber structures. Proceeding of international Symposium on Timber Structures, Istanbul, Turkey, 25-27 June 2009, 151-162.